Solid State Communications 252 (2017) 40–45

Contents lists available at ScienceDirect

Solid State Communications

journal homepage: www.elsevier.com/locate/ssc

Communication

Prediction on technetium triboride from first-principles calculations

Xiaojia Miao[a], Wandong Xing[a], Fanyan Meng[a,*], Rong Yu[b]

[a] Department of Physics, University of Science and Technology Beijing, Beijing 100083, China
[b] Key Laboratory of Advanced Materials of Ministry of Education of China, School of Materials Science and Engineering, Tsinghua University, Beijing 100084, China

ARTICLE INFO

Keywords:
Phase stability
Electronic structure
Elastic properties
Convex hull

ABSTRACT

Taking the Tc-B binary system as an example, here we report the first-principles prediction on new phases of technetium borides, TcB_3, which has an unprecedented stoichiometry. Crystal structures, phase stability, electronic properties and mechanical properties of TcB_3 have been investigated using first-principles calculations. The hexagonal $P\bar{6}m2$ structure (No.187) TcB_3 with a high value of hardness (29 GPa) is energetically stable against decomposition into other compounds under pressures above 4 GPa, indicating that TcB_3 can be synthesized above this pressure.

1. Introduction

Transition metal borides have attracted continuing interests due to their outstanding physical properties and wide engineering applications [1–15]. Currently, great interest for transition metal borides has emerged based on the design concept for intrinsically superhard compounds that the interaction of boron atoms into the transition metal lattices to form strong covalent bonds. The Tc-B system is a typical binary system which has many different stoichiometries. Tc_7B_3, TcB_2 and Tc_3B have been synthesized and investigated for many years [16]. Extensive experimental and theoretical investigations have been carried out for technetium borides by changing the stoichiometry [5,16–20].

Zhang et al. [21] predicted a hexagonal $P\bar{3}m1$ structure for TcB, which is energetically more favorable than the previously reported $P\bar{6}m2$ [17] and *Cmcm* structures [22]. Aydin and Simsek [18] investigated the structure, mechanical and electronic properties of TcB_2 and also showed that TcB_2 in ReB_2-type is more energetically favorable than that of the AlB_2-type and it is a hard material. Deligoz et al. [23] investigated the lattice dynamical and thermodynamical properties for TcB_2 in the OsB_2-type structure. Wang et al. [5] in their first-principles calculations, suggested that TcB_4 in WB_4 structure might be superhard materials, and Zhang et al. [24] proposed that the predicted TcB_4 with MoB_4-type structure has lower formation enthalpy than TcB_4 with both the WB_4-type [5] and MnB_4-type [25].

Transition metal compounds usually have various stoichiometries and crystal structures due to the coexistence of metallic, covalent, and ionic bonds in them, and this flexibility provides a lot of candidates for materials design [26]. Recently, WB_3, ReB_3, OsB_3, IrB_3, MoB_3, RuB_3, CrB_3, and MnB_3 have been widely investigated experimentally and theoretically [24,27–38]. Because of technetium lies to the specific position in the periodic table, however, technetium triboride TcB_3 so far has never been synthesized nor theoretically studied. In this work, we systematically investigate the crystal structure, phase stability, electronic structure, and mechanical properties of TcB_3. Because chemically related compounds may have a similar structure, eight possible TcB_3 structures based on the theoretical and experimental structures of known transition-metal compounds were investigated using first-principles calculations, including ReB_3-type (hexagonal, $P\bar{3}m1$, No.164) [30], TcP_3-type (orthorhombic, *Pnma*, No.62) [32], OsB_3-type (monoclinic, $P2_1/m$, No.11) [27], MoB_3-type (hexagonal, $R\bar{3}m$, No.166) [24], ReB_3-type (hexagonal, $P\bar{6}m2$, No.187) [29,30], WB_3-type (hexagonal, $P6_3/mmc$, No.194) [31], ReB_3-type (hexagonal, $P6_3/mmc$, No.194) [30], and MnB_3-type (monoclinic, $C2/m$, No.12) [28]. The results show that the hexagonal $P\bar{6}m2$ structure (No.187) TcB_3 is stable mechanically, dynamically, and thermodynamically, and can be synthesized at high pressures.

2. Computational methods

In this work, the density functional theory (DFT) calculations were performed using the projector-augmented wave (PAW) method [39–41], as implemented in the Vienna Ab-initio Simulation Package (VASP) code [42]. The generalized gradient approximation (GGA) [43] with the Perdew-Burke-Ernzerhof (PBE) scheme was used to describe the exchange-correlation function. Geometry optimization was carried out using the conjugate gradient algorithm. The plane-wave cutoff energy was 500 eV. The k-points were generated using the

* Corresponding author.
E-mail address: meng7707@sas.ustb.edu.cn (F. Meng).

http://dx.doi.org/10.1016/j.ssc.2017.01.012
Received 13 October 2016; Received in revised form 4 January 2017; Accepted 14 January 2017
Available online 15 January 2017

Monkhorst-Pack mesh [44]. In order to obtain equilibrium lattice parameters for the various TcB_3 phases, the total-energy calculations were performed by changing the volume of the phases together with the ionic positions and the cell shape allowed to vary. These total energies were then fitted with the Birch-Murnaghan equation of state [45–47]. The elastic constants were calculated using the universal-linear-independent coupling-strains (ULICS) method [48], which is computationally efficient and has been widely used in calculations of single-crystal elastic constants [49–53]. Based on the single-crystal elastic constants, the bulk modulus B and the shear modulus G were calculated according to the Voigt-Reuss-Hill approximation [54]. Young's modulus E and Poisson's ratio ν were obtained by the following equation:

$$E = 9BG/(3B + G) \quad (1)$$

$$\nu = (3B - 2G)/[2(3B + G)] \quad (2)$$

The estimated Vickers hardness (H_V) of these borides are relative to G and B through the empirical formula based on the Pugh modulus ratio k=G/B [55,56]:

$$H_V = 2(k^2G)^{0.585} - 3 \quad (3)$$

Phonon dispersion was calculated using density functional perturbation theory, as implemented in the PHONOPY code [57,58].

3. Results and discussion

As mentioned above, the predicted eight structures for TcB_3 are shown in Fig. 1. For comparison, the known technetium borides in the Tc-B phase diagram, i.e. TcB_2 (hexagonal, No.194), Tc_3B (orthorhombic, No.63) and Tc_7B_3 (hexagonal, No.186) are also included in the calculations. The formation enthalpy of the compound of Tc_xB_y was calculated using the following equation:

$$\Delta H = [H_{total}(Tc_xB_y) - (xH_{total}(Tc) + yH_{total}(B))]/(x + y) \quad (4)$$

where H, defined by $H = E + PV$, is the enthalpy of the corresponding

Table 1
Optimized lattice parameters a, b, and c (Å), cell volume (V in Å^3 per formula unit), and calculated formation enthalpy (ΔH in eV per atom).

Structure	a	b	c	V	ΔH
TcB_3-164(ReB_3)	2.861		4.646	32.94	−0.02
TcB_3-11(OsB_3)	4.114	2.883	5.856	34.24	−0.23
TcB_3-62(TcP_3)	11.185	2.854	4.552	36.33	−0.01
TcB_3-166(MoB_3)	5.193		9.333	36.33	−0.16
TcB_3-187(ReB_3)	2.908		4.572	33.48	−0.32
$TcB_3$194(WB_3)	5.256		5.980	35.76	−0.10
TcB3-12(MnB_3)	7.612	2.929	6.166	34.38	−0.27
TcB_3-194(ReB_3)	2.890		9.271	33.54	−0.28
TcB_2	2.897		7.461	27.12	−0.44
TcB_2[a]	2.892		7.453		
TcB_2[b]	2.877		7.421		
Tc_3B	2.911	9.236	7.212	48.48	−0.26
Tc_3B[a]	2.891	9.161	7.246		
Tc_3B[c]	2.919	9.283	7.265		
Tc_7B_3	7.482		4.851	117.58	−0.31
Tc_7B_3[a]	7.417		4.777		

[a] Ref.[16], Experiment.
[b] Ref.[18], VASP.
[c] Ref.[22], VASP.

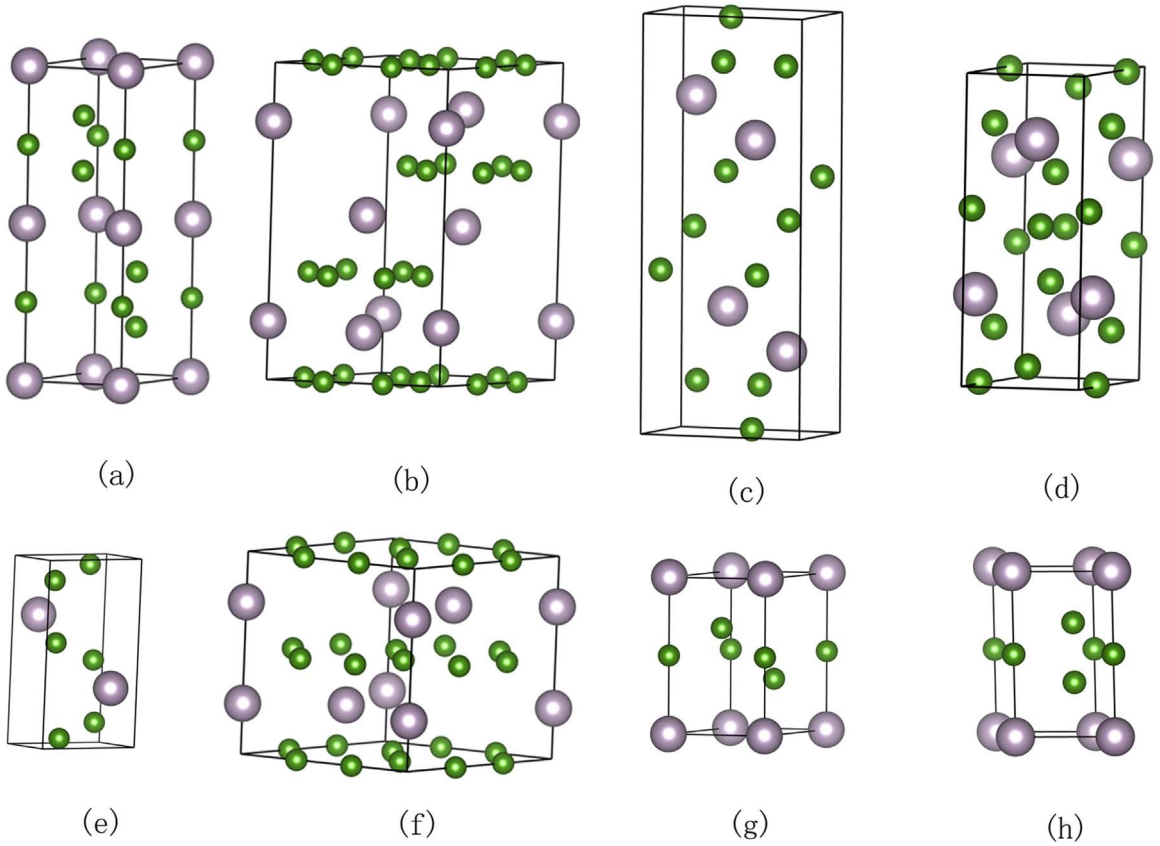

Fig. 1. Structure models of TcB_3: (a) ReB_3-type (hexagonal, No.194) : Tc 2a (0, 0, 0), B1 4f (0.3333, 0.6666, 0.6622), B2 2b (0, 0, 0.25); (b) MoB_3-type (hexagonal, No.166): Tc 6c (0, 0, 0.1849), B 18f (0.6714, 0, 0); (c) TcP_3-type (orthorhombic, No.62), Tc 4c (0.2040, 0.25, 0.1469), B1 4c (0.0159, 0.25, 0.3620), B2 4c (0.3822, 0.25, 0.3374), B3 4c (0.3877, 0.25, 0.9438); (d) MnB_3-type (monoclinic, No.12), Tc 4i (0.2878, 0, 0.7954), B1 4i (0.0067, 0, 0.7061), B2 4i (0.1741, 0, 0.4747), B3 4i (0.4348, 0, 0.1218), β=89.8518°; (e) OsB_3-type (monoclinic, No.11): Tc 2e (0.9157, 0.25, 0.6863), B1 2b (0.1911, 0.25, 0.0480), B2 2b (0.3911, 0.25, 0.5503), B3 2b (0.4889, 0.25, 0.8786), β=99.6875°; (f) WB_3-type (hexagonal, No.194): Tc1 2c (0.3333, 0.6666, 0.25), Tc2 2b (0, 0, 0.25), B 12i (0.6649, 0, 0); (g) ReB_3-type (hexagonal, No.164): Tc 1a (0, 0, 0), B1 2d (0.6666, 0.3333, 0.3334), B2 1b (0, 0, 0.5); (h) ReB_3-type (hexagonal, No.187): Tc 1a (0, 0, 0), B1 1b (0, 0, 0.5), B2 2i (0.6666, 0.3333, 0.3190). The large and small spheres represent Tc and B, respectively.

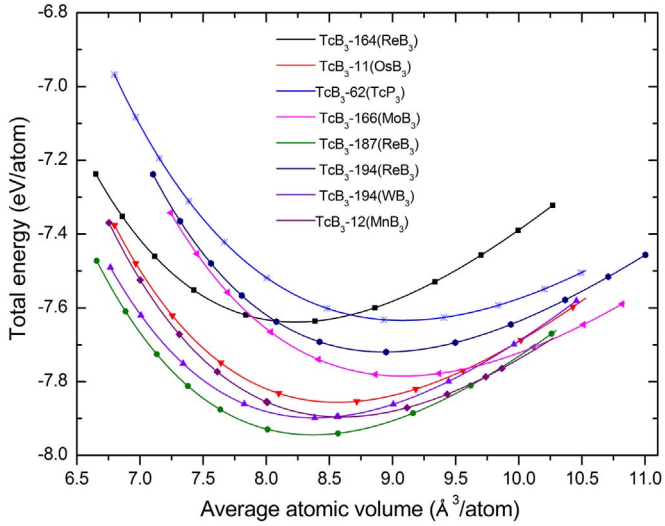

Fig. 2. The total energy-volume relationships of the eight TcB_3 phases.

compounds or elementary phases. For elemental boron, H was calculated based on the structure of α-boron [59]. The optimized lattice parameters, cell volume and formation enthalpy ΔH at zero pressure are summarized in Table 1. For the known technetium borides, our calculations are in good agreement with previous experimental and calculation values. It is worth noting that the formation enthalpies of these technetium triborides are all negative at zero pressure. The negative formation enthalpies indicate that the technetium borides are more thermodynamically stable than the mixture of elemental Tc and B at ambient condition.

The total energies of TcB_3 as a function of volume for all the phases are plotted in Fig. 2. It is clearly shown that the TcB_3-187 has the lowest energy at all the volumes. In addition, the formation enthalpies of all the TcB_3 phases have been calculated under high pressures, as shown in Fig. 3. It also suggests that the predicted TcB_3-187 is the most stable phase among the eight proposed structures at the pressure up to 100 GPa. Hereafter, only the TcB_3-187 is considered unless stated otherwise.

For a compound to be synthesized experimentally, it is more reliable to compare its enthalpy with the known compounds. Therefore, we carried out the calculations on the relative enthalpies for TcB_3-187 and the known technetium borides, i.e. TcB_2, Tc_3B and Tc_7B_3, as plotted in Fig. 4. The relative enthalpy of predicted TcB_3-187 is much lower than that of the reacting substances (Tc+3B) by 1.29 eV

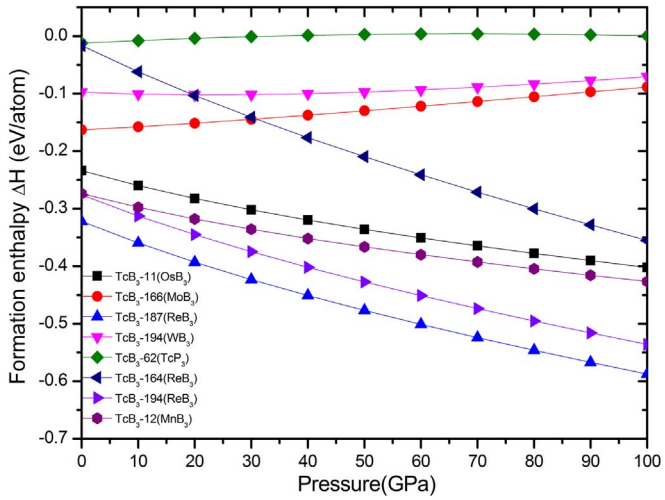

Fig. 3. Formation enthalpy-pressure diagrams for TcB_3 with eight proposed structures.

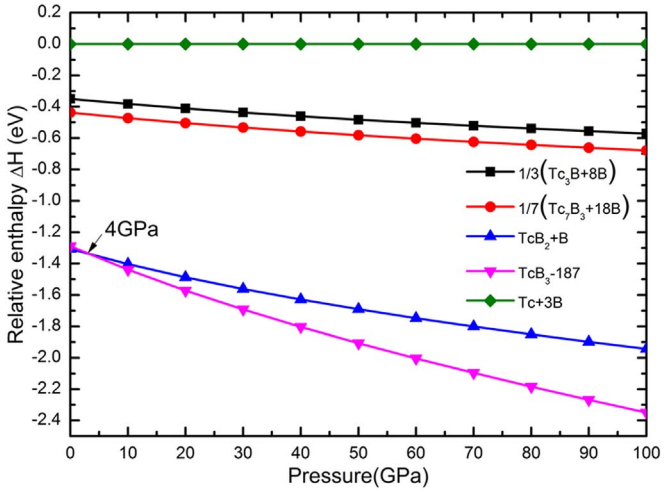

Fig. 4. The relative enthalpy-pressure diagram of technetium borides.

per formula at zero pressure. In addition, TcB_3-187 is the most energetically stable against decomposition into the mixtures of (Tc +3B), (Tc_3B+B), (Tc_7B_3+B) or (TcB_2+B) under pressure above 4 GPa, indicating that TcB_3-187 can be synthesized above this pressure.

To further validate the stability of technetium borides, we drew the convex hulls of the Tc_3B, Tc_7B_3, TcB_2, TcB-63 [22], TcB-164 [21], TcB_4 (MoB_4-type) [24] and TcB_3-187, as shown in Fig. 5. Our calculations yield a ground state convex hull at zero pressure defined by three structures: Tc_3B, Tc_7B_3, and TcB_2, which were observed experimentally [16]. However, the relative stability of various phases can be altered at high pressures. Thus, we also drew the convex hull at the pressure of 3 GPa. The predicted phases TcB-63, TcB-164, and TcB_4 (MoB_4) are found to be unstable or metastable since their enthalpies are above of the tie lines in the convex hull, as shown in Fig. 5(b). Importantly, TcB_3-187 lies on the tie line of convex hull, indicating that it is a thermodynamically stable phase. This is consistent with the results of the calculations on the relative enthalpies.

The elastic properties of materials are very important as they can provide a deeper insight into the mechanical stability, strength, hardness, and fracture toughness. The calculated elastic constants C_{ij}, bulk modulus B, shear modulus G, Young's modulus E, Poisson's ratio ν, minimum elastic eigenvalue λ_1, hardness H_V and B/G ratio of these technetium borides are given in Table 2 together with the previous computational results for comparison. The calculated values of TcB_2, Tc_3B, Tc_7B_3 and TcB_4 (MoB_4-type) in this work agree well with the previous calculation values, which underlines the accuracies of our calculations.

The TcB_3-187 is hexagonal. For a hexagonal system, the mechanical stability criteria are given by $C_{44} > 0$, $C_{11} > |C_{12}|$, and $(C_{11}+C_{12})C_{33} > 2C_{13}C_{13}$ [60]. The elastic constants of the TcB_3-187 satisfy these stability conditions, indicating that it is mechanically stable. The TcB_3-187 also has the large value of B, G, E and a high hardness of 29 GPa, demonstrating it's difficult to be compressed.

The Pugh's ratio B/G has usually been used to estimate the brittleness of materials [61,62]. Roughly, a ratio larger than 1.75 indicates that the material is ductile, otherwise it is brittle. The calculated B/G ratios for Tc_3B, Tc_7B_3 are 2.49, 2.31, respectively, indicating that they are ductile. The Pugh's ratios of TcB_3-187, TcB_2 and MoB_4-type TcB_4 are well below the critical value 1.75, suggesting that they are brittle.

We also calculated the elastic properties of TcB_3-187 at pressure of 5 GPa. The data is given in Table 3. It is seen that the elastic constants of TcB_3-187 under high pressure also satisfy the stability conditions. The elastic moduli B, G, E, and the hardness value H_V are larger at 5 GPa than at 0 GPa. The Pugh's ratio of TcB_3-187 at 5 GPa is also well below the critical value, indicating that it is still brittle at the high

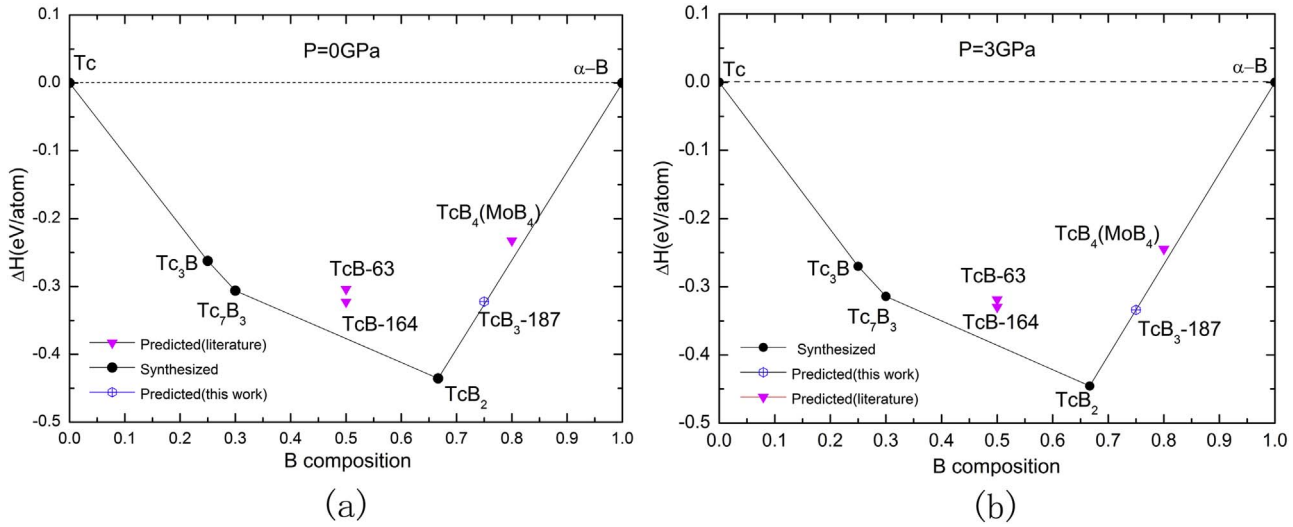

Fig. 5. The convex hulls of the Tc–B system at pressure of (a) 0 GPa (b) 3 GPa. The solid line denotes the ground state convex hull.

Table 2
Calculated elastic constants C_{ij} (GPa), bulk modulus B (GPa), shear modulus G (GPa), Young's modulus E (GPa), Poisson's ratio ν, the minimum elastic eigenvalue λ_1 (GPa), hardness H_V (GPa) and B/G ratio of technetium borides at ambient conditions.

Structure	C_{11}	C_{12}	C_{13}	C_{22}	C_{23}	C_{33}	C_{44}	C_{55}	C_{66}	B	G	E	ν	λ_1	H_V	B/G
TcB_3	503	135	152			806	221		184	292	213	515	0.21	184	29	1.37
TcB_2	557	166	97			936	249		195	303	244	578	0.18	195	36	1.24
TcB_2[a]	595	142	96			937	251			306	260	608	0.17			1.18
Tc_3B	479	214	225	486	233	456	55	204	172	307	123	326	0.32	55	8.5	2.49
Tc_3B[b]	488	219	226	503		475	63	208	181	309	141	367	0.30			2.19
Tc_7B_3	500	213	215			481	121		144	308	133	349	0.31	121	10	2.31
Tc_7B_3[b]	507	214	222			487	123			313	150	388	0.29			2.09
$TcB_4(MoB_4)$	539	110	100			938	181		214	285	222	528	0.19	181	32	1.29
$TcB_4(MoB_4)$[c]	532	115	117			912	194			288	222	530	0.19		22	1.29

[a] Ref.[18], VASP.
[b] Ref.[22], VASP.
[c] Ref.[24], VASP.

Table 3
The elastic properties of TcB_3-187 at ambient conditions and high pressure.

Structure	C_{11}	C_{12}	C_{13}	C_{33}	C_{44}	C_{66}	B	G	E	ν	λ_1	H_V	B/G
TcB_3-187 (0 GPa)	503	135	152	806	221	184	292	213	515	0.21	184	29	1.37
TcB_3-187 (5 GPa)	547	169	127	918	240	189	312	234	561	0.20	189	32	1.33

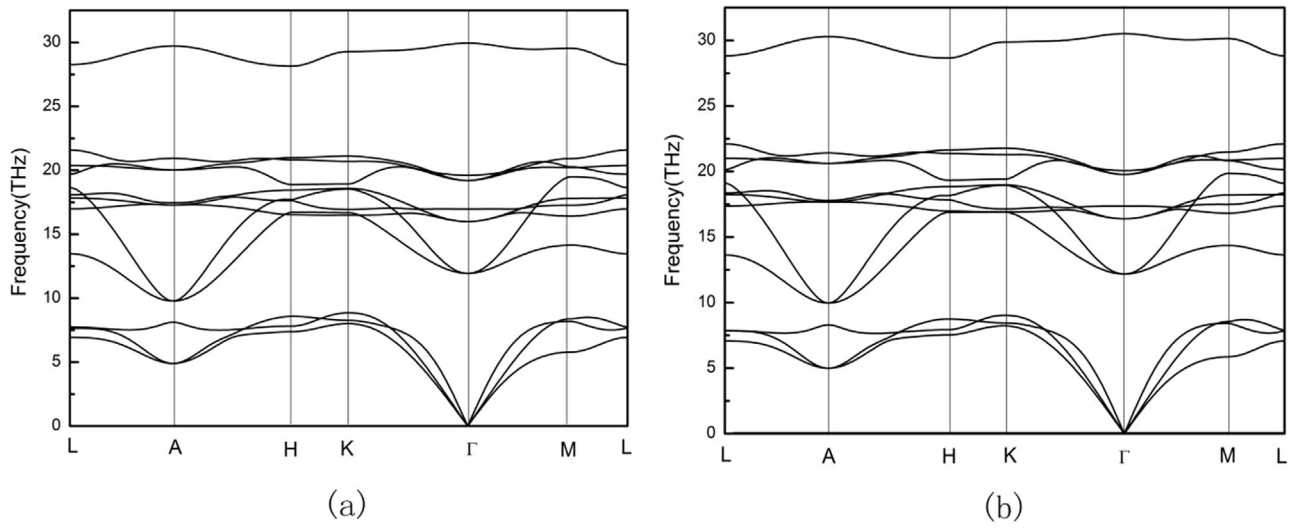

Fig. 6. Phonon dispersion curves of TcB_3-187 at pressure of (a) 0 GPa and (b) 5 GPa.

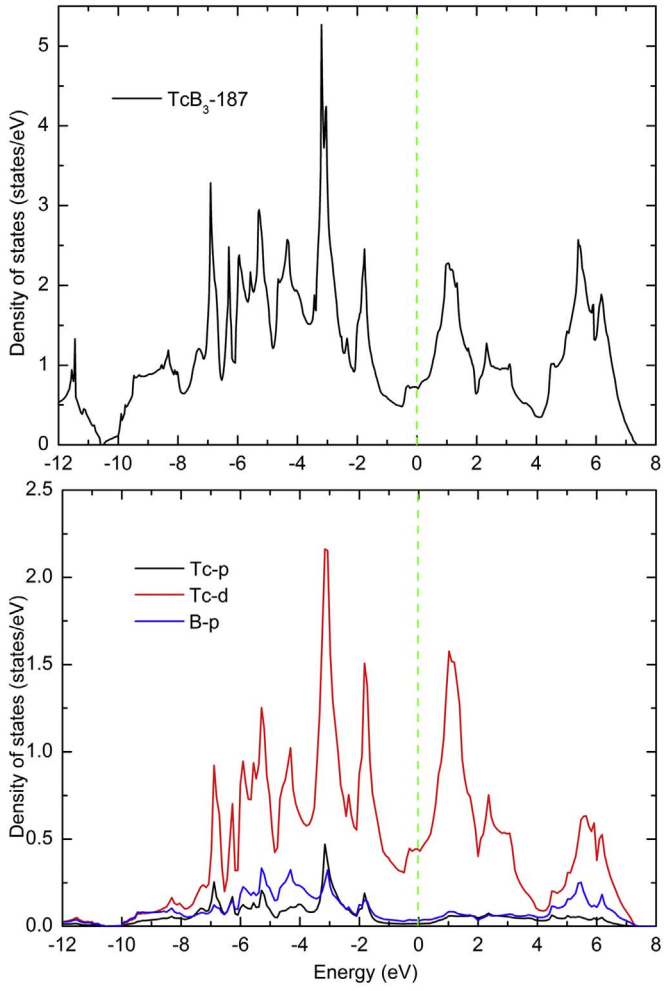

Fig. 7. Total and partial DOSs of TcB_3-187. The Fermi level is set at zero.

pressure. While the Pugh's ratio has been used in this work to estimate the brittleness of TcB_3-187, we note that Ogata and Li proposed another scale to characterize the brittleness or toughness of materials [63]. Compared to the Pugh's ratio, which is based on the elastic response of a crystal to small bond distortion, the Ogata-Li's scale considers the elastic energy density needed to spontaneously break bonds in shear and tensile strains, and correlates better to the toughness of materials than the Pugh's ratio [63]. It would be interesting to investigate the toughness of the material in further works employing the Ogata-Li's scale.

The phonon dispersion curves of TcB_3-187 at pressure of 0 GPa and 5 GPa were calculated to verify the dynamical stability, as shown in Fig. 6. A dynamically stable crystal structure requires that all phonon frequencies should be positive [64], it is clear that no imaginary phonon frequency can be found in the whole Brillouin zone, indicating that the TcB_3-187 is dynamically stable at both ambient conditions and high pressure.

In order to explain the origin of the stability and the exceptional mechanical properties of the TcB_3-187, the total and partial density of states (DOS) of TcB_3-187 were plotted in Fig. 7, where the position of the Fermi level is chosen as the reference energy zero. It's metallic with non-zero value at the Fermi level from the total DOS. This metallicity might make it a better candidate for hard conductors. It is seen that the partial DOS profiles of Tc-4*d* and B-2*p* are very similar in the range from −7.5 to 7.5 eV, indicating that the Tc-4*d* orbital has a strong hybridization with the B-2*p* orbital. The presence of a deep valley near the Fermi level (namely pseudogap) can be confirmed in our calculated DOS for TcB_3-187, which leads to a separation of the bonding and antibonding state [65,66], which will be responsible for the relative stability of TcB_3-187.

4. Conclusions

In summary, the crystal structure, phase stability, mechanical properties, and electronic structure of TcB_3 have been investigated using first-principles calculations. It is demonstrated that the hexagonal $P\bar{6}m2$ structure (No.187) TcB_3 is a hard material (H_V=29 GPa) and mechanically, dynamically, and thermodynamically stable. The predicted TcB_3-187 phase can be synthesized under pressures above 4 GPa according to the relative enthalpy between TcB_3-187 and the reacting substance of (TcB_2+B).

Acknowledgements

This work was supported by National Basic Research Program of China (2011CB606406), Fund of Key Laboratory of Advanced Materials of Ministry of Education (No. 2016AML05), the Fundamental Research Funds for the Central Universities (TP-A3:06108170), and NSFC (51371102, 51390475, 51525102). This work used the resources of Shanghai Supercomputer Center and National Center for Electron Microscopy in Beijing.

References

[1] H.Y. Chung, M.B. Weinberger, J.B. Levine, A. Kavner, J.M. Yang, S.H. Tolbert, R.B. Kaner, Science 316 (2007) 436–439.
[2] R.W. Cumberland, M.B. Weinberger, J.J. Gilman, S.M. Clark, S.H. Tolbert, R.B. Kaner, J. Am. Chem. Soc. 127 (2005) 7264–7265.
[3] X. Zhang, G.E. Hilmas, W.G. Fahrenholtz, Mater. Lett. 62 (2008) 4251–4253.
[4] Q. Gu, G. Krauss, W. Steurer, Adv. Mater. 20 (2008) 3620–3626.
[5] M. Wang, Y. Li, T. Cui, Y. Ma, G. Zou, Appl. Phys. Lett. 93 (2008) 101905.
[6] J.B. Levine, S.L. Nguyen, H.I. Rasool, J.A. Wright, S.E. Brown, R.B. Kaner, J. Am. Chem. Soc. 130 (2008) 16953–16958.
[7] J. Qin, D. He, J. Wang, L. Fang, L. Lei, Y. Li, J. Hu, Z. Kou, Y. Bi, Adv. Mater. 20 (2008) 4780–4783.
[8] J.V. Rau, A. Latini, Chem. Mater. 21 (2009) 1407–1409.
[9] X. Li, Y. Tao, F. Peng, J. Alloy. Compd. 687 (2016) 579–585.
[10] A. Latini, J.V. Rau, R. Teghil, A. Generosi, V.R. Albertini, ACS Appl. Mater. Interfaces 2 (2010) 581–587.
[11] M.M. Zhong, X.Y. Kuang, Z.H. Wang, P. Shao, L.P. Ding, X.F. Huang, J. Alloy. Compd. 581 (2013) 206–212.
[12] M. Xie, R. Mohammadi, Z. Mao, M.M. Armentrout, A. Kavner, R.B. Kaner, S.H. Tolbert, Phys. Rev. B 85 (2012) 064118.
[13] X.L. Wu, X.L. Zhou, J. Chang, Int. J. Mod. Phys. B 29 (2015) 1550103.
[14] M. Xie, R. Mohammadi, C.L. Turner, R.B. Kaner, A. Kavner, S.H. Tolbert, Phys. Rev. B 90 (2014) 104104.
[15] L. Xiong, J. Liu, L. Bai, Y. Li, C. Lin, D. He, F. Peng, J.F. Lin, J. Appl. Phys. 113 (2013) 033507.
[16] W. Trzebiatowski, J. Rudzinski, J. Less Common Met. 6 (1964) 244–245.
[17] J. Li, X. Wang, K. Liu, Y. Sun, L. Chen, H. Yang, Physica B 405 (2010) 4659–4663.
[18] S. Aydin, M. Simsek, Phys. Rev. B 80 (2009) 134107.
[19] M.M. Zhong, X.Y. Kuang, Z.H. Wang, P. Shao, L.P. Ding, X.F. Huang, J. Phys. Chem. C 117 (2013) 10643–10652.
[20] M. Zhang, H. Yan, Q. Wei, H. Wang, Comput. Mater. Sci. 68 (2013) 371–378.
[21] G.T. Zhang, T.T. Bai, H.Y. Yan, Y.R. Zhao, Chin. Phys. B 24 (2015) 106104.
[22] J.H. Wu, G. Yang, Comput. Mater. Sci. 82 (2014) 86–91.
[23] E. Deligoz, K. Colakoglu, H.B. Ozisik, Y.O. Ciftci, Solid State Sci. 14 (2012) 794–800.
[24] M. Zhang, H. Wang, H. Wang, T. Cui, Y. Ma, J. Phys. Chem. C 114 (2010) 6722–6725.
[25] W.J. Zhao, B. Xu, Comput. Mater. Sci. 65 (2012) 372–376.
[26] W.D. Xing, F.M. Meng, R. Yu, Sci. Rep. 21794 (2016) 1–9.
[27] Y. Wang, T. Yao, L.M. Wang, J. Yao, H. Li, J. Zhang, H. Gou, Dalton Trans. 42 (2013) 7041–7050.
[28] H. Niu, X.Q. Chen, W. Ren, Q. Zhu, A.R. Oganov, D. Li, Y. Li, Phys. Chem. Chem. Phys. 16 (2014) 15866–15873.
[29] X. Zhao, M.C. Nguyen, C.Z. Wang, K.M. Ho, J. Phys.: Condens. Matter 26 (2014) 455401.
[30] Q. Yan, Y.X. Wang, B. Wang, J. Yang, G. Yang, RSC Adv. 5 (2015) 25919–25928.
[31] R.F. Zhang, D. Legut, Z.J. Lin, Y.S. Zhao, H.K. Mao, S. Veprek, Phys. Rev. Lett. 108 (2012) 255502.
[32] R. Rühl, W. Jeitschko, Acta Crystallogr. 38 (1982) 2784–2788.
[33] B. Wang, X. Li, Y.X. Wang, Y.F. Tu, J. Phys. Chem. C 115 (2011) 21429–21435.
[34] M.M. Zhong, X.Y. Kuang, Z.H. Wang, P. Shao, L.P. Ding, X.F. Huang, J. Chem. Phys. 139 (2013) 234503.
[35] X.Z. Zhang, E. Zhao, Z.J. Wu, K. Li, Q. Hou, Comput. Mater. Sci. 95 (2014)

377–383.
[36] E.J. Zhao, J.P. Wang, J. Meng, Z. Wu, J. Comput. Chem. 31 (2009) 1904–1910.
[37] H.Y. Gou, Z.B. Wang, J.W. Zhang, S.T. Yan, F. Gao, Inorg. Chem. 48 (2009) 581–587.
[38] Z.W. Ji, C.H. Hu, D.H. Wang, Y. Zhong, J. Yang, W.Q. Zhang, H.Y. Zhou, Acta Mater. 60 (2012) 4208–4217.
[39] P.E. Blöchl, Phys. Rev. B 50 (1994) 17953–17979.
[40] G. Kresse, D. Joubert, Phys. Rev. B 59 (1999) 1758.
[41] P. Hohenberg, W. Kohn, Phys. Rev. 136 (1964) B864–B871.
[42] G. Kresse, J. Furthmüller, Phys. Rev. B 54 (1996) 11169.
[43] J.P. Perdew, K. Burke, M. Ernzerhof, Phys. Rev. Lett. 77 (1996) 3865.
[44] H.J. Monkhorst, J.D. Pack, Phys. Rev. B 13 (1976) 5188–5192.
[45] F. Murnaghan, P. Natl. Acad. Sci. 30 (1944) 244–247.
[46] F. Birch, J. Geophys. Res. 57 (1952) 227–286.
[47] F. Birch, Phys. Rev. 71 (1947) 809–824.
[48] R. Yu, J. Zhu, H.Q. Ye, Comput. Phys. Commun. 181 (2010) 671–675.
[49] C. Wei, J.L. Fan, H.R. Gong, J. Alloy. Compd. 618 (2015) 615–622.
[50] Y.T. Hu, H. Gong, J. Alloy. Compd. 639 (2015) 635–641.
[51] M. Bartosik, M. Todt, D. Holec, J. Todt, L. Zhou, H. Riedl, H.J. Böhm, F.G. Rammerstorfer, P.H. Mayrhofer, Appl. Phys. Lett. 107 (2015) 071602.
[52] D. Holec, F. Tasnádi, P. Wagner, M. Friák, J. Neugebauer, P.H. Mayrhofer, J. Keckes, Phys. Rev. B 90 (2014) 184106.
[53] D.Y. Dang, J.L. Fan, H.R. Gong, J. Appl. Phys. 116 (2014) 033509.
[54] B. Karki, L. Stixrude, S. Clark, M. Warren, G. Ackland, J. Crain, Am. Mineral. 82 (1997) 51–60.
[55] X.Q. Chen, H. Niu, C. Franchini, D. Li, Y. Li, Phys. Rev. B 84 (2011) 121405.
[56] X.Q. Chen, H. Niu, D. Li, Y. Li, Intermetallics 19 (2011) 1275–1281.
[57] A. Togo, F. Oba, I. Tanaka, Phys. Rev. B 78 (2008) 134106.
[58] S. Baroni, S. De Gironcoli, A. Dal Corso, P. Giannozzi, Rev. Mod. Phys. 73 (2001) 515.
[59] G. Will, B. Kiefer, Z. Anorg, Allg. Chem. 627 (2001) 2100–2104.
[60] Z.J. Wu, E.J. Zhao, H.P. Xiang, X.F. Hao, X.J. Liu, J. Meng, Phys. Rev. B 76 (2007) 054115.
[61] S.F. Pugh, Philos. Mag. 45 (1954) 823–843.
[62] L. Vitos, P.A. Korzhavyi, B. Johansson, Nat. Mater. 2 (2003) 25–28.
[63] S. Ogata, J. Li, J. Appl. Phys. 106 (2009) 113534.
[64] L. Zhou, F. Körmann, D. Holec, M. Bartosik, B. Grabowski, J. Neugebauer, P.H. Mayrhofer, Phys. Rev. B 90 (2014) 184102.
[65] R. Yu, L.L. He, H.Q. Ye, Phys. Rev. B 65 (2002) 184102.
[66] R. Hoffmann, Solids and Surfaces, VCH Publisher, New York, 1988.